IEEE Photonics Journal
An IEEE Photonics Society Publication

Open Access

Unraveling the Enhanced Electrical Conductivity of PEDOT:PSS Thin Films for ITO-Free Organic Photovoltaics

Volume 6, Number 4, August 2014

Sheng Hsiung Chang
Chien-Hung Chiang
Feng-Sheng Kao
Chuen-Lin Tien
Chun-Guey Wu

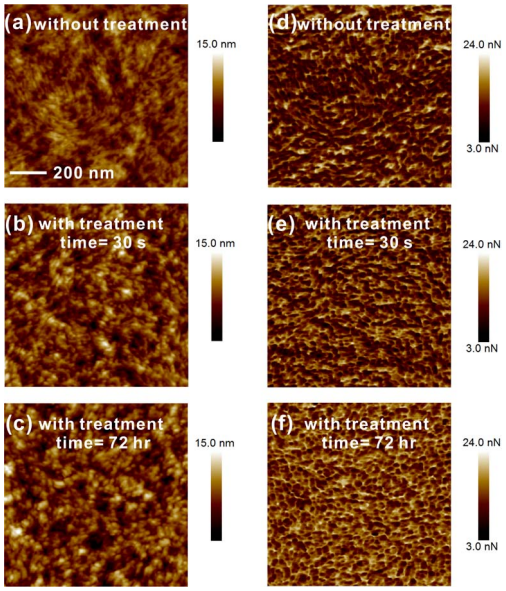

DOI: 10.1109/JPHOT.2014.2331254
1943-0655 © 2014 IEEE

IEEE photonics SOCIETY

IEEE

Unraveling the Enhanced Electrical Conductivity of PEDOT:PSS Thin Films for ITO-Free Organic Photovoltaics

Sheng Hsiung Chang,[1] Chien-Hung Chiang,[1] Feng-Sheng Kao,[2] Chuen-Lin Tien,[3] and Chun-Guey Wu[1]

[1]Research Center for New Generation Photovoltaics, National Central University, Jongli 32001, Taiwan
[2]Industrial Technology Research Institute, Hsinchu, Taiwan
[3]Institute of Electrical Engineering, Feng Chia University, Taichung 40724, Taiwan

DOI: 10.1109/JPHOT.2014.2331254

Manuscript received May 15, 2014; revised June 3, 2014; accepted June 4, 2014. Date of current version July 9, 2014. This work was supported by the National Science Council under Grant NSC 101-2731-M-008-002-MY3. Corresponding author: S. H. Chang (e-mail: shchang@ncu.edu.tw).

Abstract: We present the structure and the optical and mechanical properties of highly conductive PEDOT:PSS (1:2.5 wt%, PH1000) thin films fabricated with and without an immersion treatment process using a solution containing 67% ethylene glycol and 33% hexafluoro-isopropyl alcohol, by volume. The enhanced electrical conductivity of the PEDOT:PSS thin films originated from the formation of a conducting PEDOT network in combination with an increased electron concentration due to the conformational changes in the PEDOT chains. The modified PEDOT:PSS thin film was used as a transparent anode electrode for P3HT:PCBM blended film-based photovoltaics, resulting in a power conversion efficiency of 3.28% under 1-sun illumination.

Index Terms: Optoelectronic materials, organic materials, photovoltaics.

1. Introduction

The performance of transparent conducting films (TCFs) is crucial for ensuring the efficiency of optoelectronic devices, such as light-emitting diodes, laser diodes, liquid-crystal displays, photodetectors, and photovoltaics. The development of TCFs with high transmittance and low resistivity is an important issue. Tin-doped indium oxide (ITO) and modified Ga-doped zinc oxide (GZO) [1], [2] have been widely used as the anode and cathode electrodes, respectively. Usually, a thermal annealing process is required to achieve low resistivity and high transparency in the visible range [3]–[5]. However, the flexible plastic substrate can be damaged by thermal annealing at temperatures above 200 °C, which is why it is important to fabricate TCFs at low temperatures. Poly(3,4-ethylenedioxythiophene) (PEDOT) is one of the more promising candidates for light transmission and hole extraction (injection). The highest electrical conductivity reported for PEDOT thin film is obtained using the vacuum vapor-phase polymerization technique and it is about 3400 S/cm [6]. It has been demonstrated that high conductivities of poly(3,4-ethylenedioxythiophene):poly(styrene sulfonate) (PEDOT:PSS) thin films can be obtained through a solution process which involves adding a solvent additive and/or conducting post treatment at low temperatures [7]–[10]. The electrical conductivity of PEDOT:PSS thin films is quite low, which has been explained as due to the disconnected PEDOT chains. The electrical conductivity of

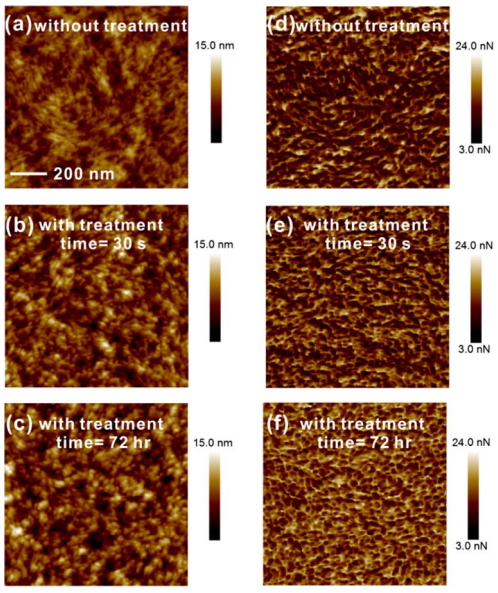

Fig. 1. Atomic force microscopy images of PEDOT:PSS thin films. (a)–(c) Images of the topography. (d)–(f) Adhesion images. The length of scale bar is 200 nm.

PEDOT:PSS (1:2.5 wt%) thin film can be enhanced from 0.3 S/cm to 1362 S/cm due to the removal of insulator PSS and the formation of interconnected conducting PEDOT chains [11]. Recently, The electrical conductivity of PEDOT:PSS thin films has been increased from 0.3 S/cm to 3300 S/cm by treatment with methanesulfonic acid [12]. The morphology, ultraviolet-to-visible optical transmittance, and spectroelectrochemical responses of PEDOT:PSS thin films have been investigated in order to obtain a fundamental understanding of the processes involved [7], [12]–[14]. However, the enhanced conductivity of PEDOT:PSS thin films has not yet been quantitatively analyzed. The goal of this study is to understand the enhanced conductivity of PEDOT:PSS thin films fabricated with an immersion treatment process.

2. Experiments

A PEDOT:PSS (1:2.5 wt%) aqueous solution (Heraeus Co.) was spin-coated onto the glass substrate at a spin speed of 1500 rpm for 50 s. The PEDOT:PSS thin films were subsequently annealed on a hot plate at 120 °C for 10 min in the ambient atmosphere. The films were immersed in a solution containing 67% ethylene glycol (EG) and 33% hexafluoro-isopropyl alcohol (HFIP), by volume. The functions of EG and HFIP have been investigated in [15]. Then the treated films were annealed again on a hot plate at 120 °C for 10 min. The near-infrared transmittance of the PEDOT:PSS thin films was analyzed by the Maxwell Garnett model [16] to obtain the carrier concentration and local conductivity. The removal of PSS and conformational change in the PEDOT chains were observed by Raman spectroscopy.

3. Analysis

Fig. 1 presents the topography and adhesion images of the PEDOT:PSS thin films. Compared with the phase images of PEDOT:PSS thin films in [11], [17], the bright region (white) and dark region (brown) of adhesion images can be assigned as the PEDOT and PSS, respectively. After the immersion treatment, the elongated shape changed to become more sphere-like, which means that the PSS was partially removed. The adhesion images show that the removal of PSS results in the formation of a conducting PEDOT network, which has a great benefit to the enhancement of electrical conductivity.

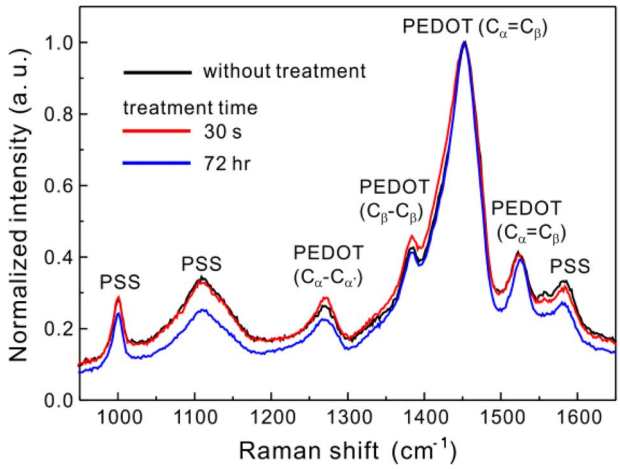

Fig. 2. Raman spectra of PEDOT:PSS thin films with and without an immersion treatment process.

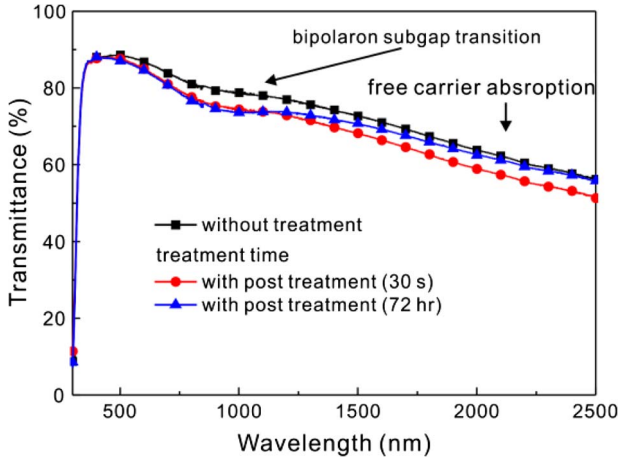

Fig. 3. Transmittance spectra of PEDOT:PSS thin films.

Fig. 2 presents the Raman spectra of the PEDOT:PSS thin films under green light excitation $(= 532\ \text{nm})$. The Raman fingerprints of PEDOT and PSS have been investigated in [13], [18], [19]. The vibrational modes of PEDOT are located at 1524 cm^{-1}, 1452 cm^{-1}, 1383 cm^{-1}, and 1272 cm^{-1}, and assigned to the $C_\alpha = C_\beta$ asymmetrical, $C_\alpha = C_\beta$ symmetrical, $C_\beta - C_\beta$ stretching, and $C_\alpha - C_{\alpha'}$ inter-ring stretching vibrations, respectively. The vibrational modes of PSS are located at 1110 cm^{-1} and 1000 cm^{-2}. There is a Raman shift of 1383 cm^{-1} (1272 cm^{-1}), indicating a reduction in the intensity so that the $C_\alpha - C_{\alpha'}$ $(C_\beta - C_\beta)$ changes to $C_\alpha = C_{\alpha'}$ $(C_\beta = C_\beta)$. As a consequence, the conformation of the PEDOT changes from a benzoid structure (coil conformation) to a quinoid structure (linear conformation) after an immersion treatment process for 72 hrs. On the other hand, the partial removal of PSS is observed by the reduction in intensity of the Raman fingerprints. Before that, the reduction of PSS has been confirmed by x-ray photoelectron spectroscopy [9], [11], [12], [17].

Fig. 3 presents the visible-to-near-infrared transmittance spectra of PEDOT:PSS thin films. The average transmittance of the PEDOT:PSS thin films is higher than 85% in visible range. In the near-infrared range, the lower transmittance of the PEDOT:PSS thin films is due to the bipolaron subgap transition (BST) and the free carrier effect of the PEDOT. After an immersion treatment, the red-shift in the BST indicates an increase in the carrier concentration of the PEDOT. The BST is the photo-excited electron transition from the Fermi level to the energy level within

TABLE 1

Thickness, volume ratio, carrier concentration, local conductivity and electrical conductivity of PEDOT:PSS thin films

Sample number	Treatment time	Thickness (nm)	Volume ratio	Carrier concentration (cm^{-3})	Local conductivity (S/cm)	Electrical conductivity (S/cm)
1	0	54	1:2.50	5.04×10^{20}	944	0.84
2	30 s	43	1.1.79	7.30×10^{20}	1140	385
3	72 hr	33	1:1.14	8.23×10^{20}	1284	1210

the electrical band gap [20]. Therefore, the red-shifted BST corresponds to conformational change of the PEDOT chains from a benzoid structure (de-doping state) to a quinoid structure (doping state).

The local carrier concentration and mobility of PEDOT can be determined by fitting the transmittance of the PEDOT:PSS/glass with the transfer matrix method. The Maxwell Garnett model was used to calculate the effective refractive index, in order to separate the contribution of PEDOT from PEDOT:PSS thin film. Before fitting the experimental curves, the film thickness and volume ratio of PEDOT in the blended thin films has to be known. The thickness of the PEDOT:PSS thin films was measured by an α-step (Veeco Dektak 150). There was increase in the volume ratio between PEDOT and PSS due to the partial removal of PSS. Here, the amount of PEDOT was assumed to be fixed. The measured thickness and the estimated volume ratio of the PEDOT:PSS thin film are listed in Table 1. The dielectric constant of the insulator PSS is assumed to be 2.56 [8]. The dielectric constant of the conducting PEDOT is described by the Drude model as follows:

$$\varepsilon_{PEDOT}(\omega) = \varepsilon_\infty - \frac{\omega_p^2}{\omega(\omega + j\nu_c)} \tag{1}$$

where ε_∞ is assumed to be 2.56 [8], ω_p is the plasma frequency of free carrier, and ν_c is the collision frequency of free carrier. The carrier concentration (N) and local conductivity (σ) can be calculated by $N = \varepsilon_0 m^* \omega_p^2 / e^2$ and $\sigma = \varepsilon_0 \omega_p^2 / \nu_c$, respectively, where ε_0 is the absolute permittivity, the effective carrier mass, m^*, is assumed as $0.3m_e$ [21], m_e is the electron mass, and e is the electric charge. The local conductivity is the so called Drude direct current conductivity. The PEDOT:PSS thin film is a nanocomposite material as shown in Fig. 1. Therefore, the average dielectric response of the thin film can be described by the Maxwell Garnett model, and the depolarization factor is 1/3 due to the sphere-like PEDOT nanoparticles. Fig. 4 shows the transmittance spectrum of the PEDOT:PSS/glass fitted with the transfer matrix method to obtain the carrier concentration and local conductivity of PEDOT. Here, an error function is defined as follows:

$$EF = \sum_{\lambda=1500\,\mathrm{nm}}^{2500\,\mathrm{nm}} \frac{\left|T_{fit}(\lambda) - T_{\exp}(\lambda)\right|}{1001\,T_{\exp}(\lambda)} \tag{2}$$

where λ is wavelength, $T_{\exp}$ is the transmittance of PEDOT:PSS thin films, and T_{fit} is the fitted transmittance. The all values of EF are smaller than 0.002 in Fig. 4. In addition, a four-point probe (FPP) was used to determine the electrical conductivity of the PEDOT:PSS thin films. In the first 30 s of treatment, the electrical conductivity was dramatically enhanced from 0.84 S/cm to 385 S/cm. After undergoing treatment for 72 hrs, the electrical conductivity (1210 S/cm) became quite close to the local conductivity (1284 S/cm), which means that carrier transport in the connected PEDOT network was nearly free.

In order to understand the mechanical properties of PEDOT:PSS thin films fabricated with and without an immersion treatment process, a home-made Twyman-Green interferometer [22]

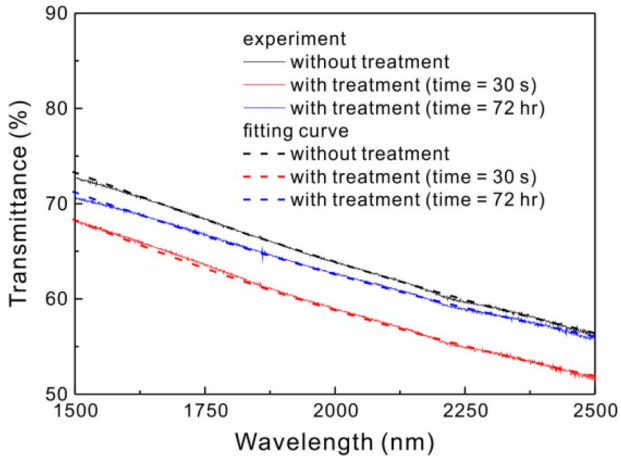

Fig. 4. Solid lines are the transmittance spectra of the PEDOT:PSS thin films; the dashed lines are the fitting curves.

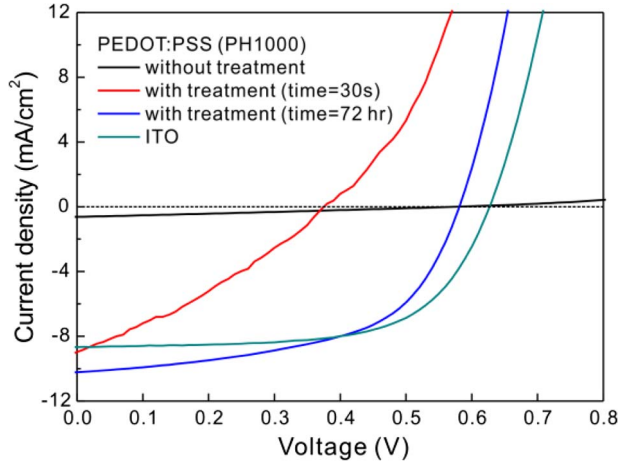

Fig. 5. Current density-voltage curves of P3HT:PCBM blended film based photovoltaics for different transparent anode electrodes.

was used to measure the residual stress. Usually, the negative (compressive) and positive (tensile) residual stresses correspond to the dense and diluted phases, respectively [23], [24]. In the first 30 s of treatment, the residual stress of the PEDOT:PSS thin film was inverted from compressive stress (−0.061 GPa) to tensile stress (0.957 GPa) due to the partial removal of PSS. After 72 hours of immersion treatment, there was a significant reduction in the initially induced tensile stress in the PEDOT:PSS thin film from 0.957 GPa to 0.316 GPa. In the Raman spectra (Fig. 2), the width of the prominent peak (C=C) decreases when treatment is changed from 30 s to 72 hrs. It means that the crystallinity of PEDOT was improved after 72 hrs of immersion treatment. Therefore, the reduction of the tensile stress may be originated from the enhanced crystallinity of PEDOT. The low residual stress corresponds to the high electrical conductivity in the PEDOT:PSS thin films fabricated with an immersion treatment process due to the denser PEDOTs.

4. Photovoltaic Performances

The PEDOT:PSS thin films were used to produce a transparent anode electrode for organic photovoltaics (OPVs). P3HT and PCBM with 1:1 weight ratio were dissolved in 1 mL

TABLE 2
Device performances of P3HT:PCBM blended film based photovoltaics

Anode electrode	J_{sc} (mA/cm^2)	V_{oc} (V)	FF (%)	PCE (%)
1	0.62	0.53	0.27	0.11
2	9.00	0.38	0.31	1.06
3	10.25	0.59	0.54	3.28
ITO	8.67	0.63	0.63	3.55

1,2-dichlorobenzene, and the mixture was stirred overnight. The P3HT:PCBM blended film was spin-coated on top of the PEDOT:PSS thin film with a spin speed of 500 rpm for 60s. In order to optimize the interpenetration network of the P3HT:PCBM blended films, the samples subsequently underwent solvent annealing and thermal annealing. Then, Ca and Ag were thermally evaporated onto the sample to act as the adhesion layer and the cathode electrode, respectively. The device of ITO/PEDOT:PSS(1:6 wt%, AI4083)/P3HT:PCBM/Ca/Ag was fabricated as the reference photovoltaic. The active area of the devices is 0.2 cm $\times$ 0.5 cm. The detailed fabrication process is described in our previous report [25]. The current density-voltage (J-V) curves of all devices were measured using a Keithley 4200 source-measurement unit. A calibrated solar simulator (Oriel) with 100 mW/cm^2 power density was used as the light source.

Fig. 5 presents the J-V curves of OPVs under 1-sun illumination. The device performances of P3HT:PCBM blended film based photovoltaics are listed in Table 2. The disconnected PEDOTs resulted in a small short-circuit current density (J_{sc}) and fill factor (FF) when the unmodified PEDOT:PSS thin film was used as the anode electrode. There was a significant improvement in the J_{sc} and FF of the OPV after the PEDOT:PSS thin film was treated for 72 hrs. Reference [26] can help us to understand the performance of photovoltaics. Compared with blue curve (PH1000 with treatment, treatment time $=$ 72 hr), the smaller FF and the lower J_{sc} of black curve (PH1000 without treatment) are originated from the higher resistance of photovoltaics. The high resistance of photovoltaics is due to the low electrical conductivity $(= 0.84$ S/cm$)$ of PEDOT:PSS thin film. Compared with blue curve, the smaller open-circuit voltage of red curve (PH1000 with treatment, treatment time $=$ 30 s) is due to the lower shunt resistance. Compared with green curve (ITO reference photovoltaic), the V_{oc} of blue curve is smaller due to the lower shunt resistance. The shunt resistance is defined as the slop of J-V curve at $V = 0$.

5. Conclusion

In summary, the electrical conductivity of PEDOT:PSS (1:2.5 wt%) thin films was enhanced from 0.84 S/cm to 1210 S/cm through an immersion treatment process using a solution containing 67% ethylene glycol (EG) and 33% hexafluoro-isopropyl (HFIP) alcohol, by volume. The partial removal of the insulator PSS, the formation of the connected conducting PEDOT networks, and the increased carrier concentration altogether contribute to the enhanced electrical conductivity of the PEDOT:PSS thin films. The increased carrier concentration can be explained by the conformational change of PEDOT chains from a benzoid structure (de-doping state) to a quinoid structure (doping stage), as observed from the near-infrared transmittance and Raman spectra. The partial removal of insulator PSS reflected on the intensity reduction of the Raman fingerprint and the inverted residual stress from compressive stress to tensile stress. It was demonstrated that the modified PEDOT:PSS (1:1.14 wt%) thin film could replace ITO film as a stand-alone transparent anode electrode for P3HT:PCBM blended film based photovoltaics.

References

[1] H.-K. Park, J.-W. Kang, S.-I. Na, D.-Y. Kim, and H.-K. Kim, "Characteristics of indium-free GZO/Ag/GZO and AZO/Ag/AZO multilayer electrode grown by dual target DC sputtering at room temperature for low-cost organic photovoltaics," *Sol. Energy Mater. Sol. C.*, vol. 93, no. 11, pp. 1994–2002, Nov. 2009.

[2] S.-G. Ihn *et al.*, "ITO-free inverted polymer solar cells using a GZO cathode modified by ZnO," *Sol. Energy Mater. Sol. C.*, vol. 95, no. 7, pp. 1610–1614, Jul. 2011.

[3] R. B. H. Tahar, T. Ban, Y. Ohya, and Y. Takahashi, "Tin doped indium oxide thin films: Electrical properties," *J. Appl. Phys.*, vol. 83, no. 5, pp. 2631–2645, Mar. 1998.

[4] J. Ederth *et al.*, "Electrical and optical properties of thin films consisting of tin-doped indium oxide nanoparticles," *Phys. Rev. B, Condens. Matter*, vol. 68, no. 15, pp. 155410-1–155410-10, Oct. 2003.

[5] J. H. Kim *et al.*, "Effect of rapid thermal annealing on electrical and optical properties of Ga doped ZnO thin films prepared at room temperature," *J. Appl. Phys.*, vol. 100, no. 11, pp. 113515-1–113515-3, Dec. 2006.

[6] M. V. Fabretto *et al.*, "Polymer material with metal-like conductivity of next generation organic electronic devices," *Chem. Mater.*, vol. 24, no. 20, pp. 3998–4003, Oct. 2012.

[7] J. Ouyang *et al.*, "On the mechanism of conductivity enhancement in poly(3,4-ethylenedioxythiophene):poly(styrene sulfonate) film through solvent treatment," *Polymer*, vol. 45, no. 25, pp. 8443–8450, Nov. 2004.

[8] M. Yamashita, C. Otani, M. Shimizu, and H. Okuzaki, "Effects of solvent on carrier transport in poly(3,4-ethylenedioxythiophene)/poly(4-styrenesulfonate) studied by terahertz and infrared-ultraviolet spectroscopy," *Appl. Phys. Lett.*, vol. 99, no. 14, pp. 143307, Oct. 2011.

[9] Y. Xia, K. Sun, J. Ouyang, "Solution-processed metallic conducting polymer films as transparent electrode of optoelectronic devices," *Adv. Mater.*, vol. 24, no. 18, pp. 2436–2440, May 2012.

[10] Q. Wei, M. Mukaida, Y. Naitoh, and T. Ishida, "Morphological change and mobility enhancement in PEDOT:PSS by adding co-solvents," *Adv. Mater.*, vol. 25, no. 20, pp. 2831–2836, May 2013.

[11] D. Alemu, H.-Y. Wei, K.-C. Ho, and C.-W. Chu, "Highly conductive PEDOT:PSS electrode by simple film treatment with methanol for ITO-free polymer solar cells," *Energy Environ. Sci.*, vol. 5, pp. 9662–9671, 2012.

[12] J. Ouyang, "Solution-processed PEDOT:PSS films with conductivities as indium tin oxide through a treatment with mild and weak organic acids," *Appl. Mater. Interfaces*, vol. 5, no. 24, pp. 13082–13088, Dec. 2013.

[13] S. Garreau, J. L. Duvail, and G. Louarn, "Spectroelectrochemical studies of poly(3,4-ethylenedioxythiophene) in aqueous medium," *Synthetic Metals*, vol. 125, no. 3, pp. 325–329, Dec. 2002.

[14] D. A. Mengistie, P.-C. Wang, and C.-W. Chu, "Effect of molecular weight of additives on the conductivity of PEDOT:PSS and efficiency for ITO-free organic solar cells," *J. Mater. Chem. A*, vol. 1, pp. 9907–9915, 2013.

[15] C.-H. Chiang and C.-G. Wu, "High-efficient dye-sensitized solar cell based on highly conducting and thermally stable PEDOT:PSS/glass counter electrode," *Org. Electron.*, vol. 14, no. 7, pp. 1769–1776, Jul. 2013.

[16] M. Y. Koledintseva, R. E. DuBroff, and R. W. Schwartz, "A Maxwell Garnett model for dielectric mixtures containing conducting particles at optical frequencies," *PIERS*, vol. 63, pp. 223–242, 2006.

[17] Y. H. Kim *et al.*, "Highly conductive PEDOT:PSS electrode with optimized solvent and thermal post-treatment for ITO-free organic solar cells," *Adv. Funct. Mater.*, vol. 21, no. 6, pp. 1076–1081, Mar. 2011.

[18] Y.-K. Han *et al.*, "Improved performance of polymer solar cells featuring one-dimensional PEDOT nanorods in a modified buffer layer," *J. Electrochem. Soc.*, vol. 158, no. 3, pp. K88–K93, 2011.

[19] A. A. Farah *et al.*, "Conductivity enhancement of poly(3,4-ethylenedioxythiophene)-poly(styrenesulfonate) film post-spincasting," *J. Appl. Phys.*, vol. 112, no. 11, pp. 113709-1–113709-8, Dec. 2012.

[20] J. Hwang *et al.*, "In situ measurements of the optical absorption of dioxythiophene-based conjugated polymers," *Phys. Rev. B, Condens. Matter*, vol. 83, no. 19, pp. 195121-1–195121-12, May 2011.

[21] H. B. Akkerman et al., "Electron tunneling through alkanedithiol self-assembled monolayers in large-area molecular junctions," *Proc. Nat. Acad. Sci. USA*, vol. 104, no. 27, pp. 11 161–11 166, Jul. 2007.

[22] C.-L. Tien and H.-D. Zeng, "Measuring residual stress of anisotropic thin film by fast Fourier transform," *Opt. Exp.*, vol. 18, no. 16, pp. 16594–16600, Aug. 2010.

[23] K. Srinivasarao, G. Srinivasarao, K. V. Madhuri, K. K. Murthy, and P. K. Mukhopadhyay, "Preparation and characterization of R.F. magnetron sputtered Mo:ZnO thin films," *Indian J. Mater. Sci.*, vol. 2013, pp. 684730-1–684730-7, 2013.

[24] S. Desgreniers, "High-density phases of ZnO: Structural and compressive parameters," *Phy. Rev. B, Condens. Matter*, vol. 58, no. 21, pp. 14 102–14 105, Dec. 1998.

[25] C.-G. Wu, C.-H. Chiang, and H.-C. Han, "Manipulating the horizontal morphology and vertical distribution of the active layer in BHJ-PSC with a multi-functional solid organic additive," *J. Mater. Chem. A*, vol. 2, pp. 5295–5303, 2014.

[26] B. Qi and J. Wang, "Fill factor in organic solar cells," *Phys. Chem. Chem. Phys.*, vol. 15, pp. 8972–8982, 2013.